

Better Bubble Process Modeling : Improved Bubble Hydrodynamics Parameterization

Ranjan Patro¹, Ira Leifer² and Peter Bowyer³

¹Physics Department, Memorial University of Newfoundland, St. John's, Canada

²Chemical Engineering Department, University of California, Santa Barbara, California, USA.

³Department. of Oceanography, National University of Ireland, Galway, Ireland

Proper modeling of bubble-mediated processes requires both good observations and parameterizations. Although one of the most important bubble parameterizations is the rise velocity, V_B , published studies of V_B in natural waters (i.e., sea water, marsh water, lake water) are largely unavailable; most studies are for "clean" distilled water. Also poorly studied is the effect of temperature, T on V_B .

An examination of V_B in seawater showed that for bubbles with radius, $r > 700 \mu\text{m}$, V_B was not significantly different from the value for distilled water. Analysis of V_B with depth, showed a decrease in V_B as the bubble rose over a distance, suggesting bubble contamination can take a significant time (1 m or more), and this time increases with increasing r . Also, hydrodynamic contamination was fastest in marsh and lake waters, where the water was collected close to sediments. Experiments to measure V_B over the range $0 < T < 40^\circ\text{C}$ showed that for non-oscillating bubbles, $V_B(T)$ increases with T ; while for larger bubbles, $V_B(T)$ decreases with T due to oscillations. A three-part parameterization of $V_B(r, T)$ with transitions at $Re = 1, 540$, and the onset of oscillations (itself T dependent) was developed.

1. INTRODUCTION

The bubble rise velocity, V_B , is of both academic and practical interest. Investigation of bubble behavior is important to fluid dynamics and mass transfer [Tuschiya *et al.*, 1997], oceanic noise [Medwin and Bretiz, 1989], aerosol generation [Monahan, 1986], and chemical and industrial applications [Clift *et al.*, 1978]. Several parameters affect V_B including size, temperature, T , and the presence of surface active materials, or surfactants. Although V_B is well characterized for water at 20°C and other liquids, the relationships between V_B and T and for V_B in natural waters has not been quantified. This research investigated V_B for bubbles in various natural waters and over a range of T .

2. EXPERIMENTAL SET-UP and PROCEDURE

The experimental studies were performed in a Plexiglas tank 12 cm square by 60 cm tall. Bubbles over the range $360 < r < 4500 \mu\text{m}$, where r is the equivalent spherical radius, were generated from a regulated air flow through

drawn capillary tubes inserted in a rubber stopper in one tank wall, 5 cm from the bottom. Two video cameras were used to simultaneously observe r and V_B . Images were recorded for later digitization and analysis. Analysis was by routines written in NIH Image (developed at the U.S. National Institutes of Health and available on the Internet at <http://rsb.info.nih.gov/nih-image/>) and MatLab (The MathWorks, Nantick, MA). The x, y position of each bubble, its major and minor axes (determined by a best fit ellipse), and the time were calculated for each frame. Further data analysis including outlier removal and compensation for hydrostatic changes were performed in MatLab. A detailed description of the set-up, procedure, and analysis methodology, is provided in Leifer *et al.* [2000]. V_B was measured at 20°C for various natural waters collected in polyethylene containers from locations in County Galway, Ireland at a depth of 10 cm, and then filtered.

3. RESULTS

3.1. Observation of Rise Velocity

A comparison of observed V_B at $T = 20^\circ\text{C}$ for distilled, i.e., clean, and natural waters as well as from other researchers is shown in Figure 1. Also shown is the developed V_B parameterization presented below for clean (this work) and dirty (immobilized interface) bubbles from *Clift et al. [1978]*. For clean bubbles, V_B increases with r until the onset of oscillation after which V_B decreases.

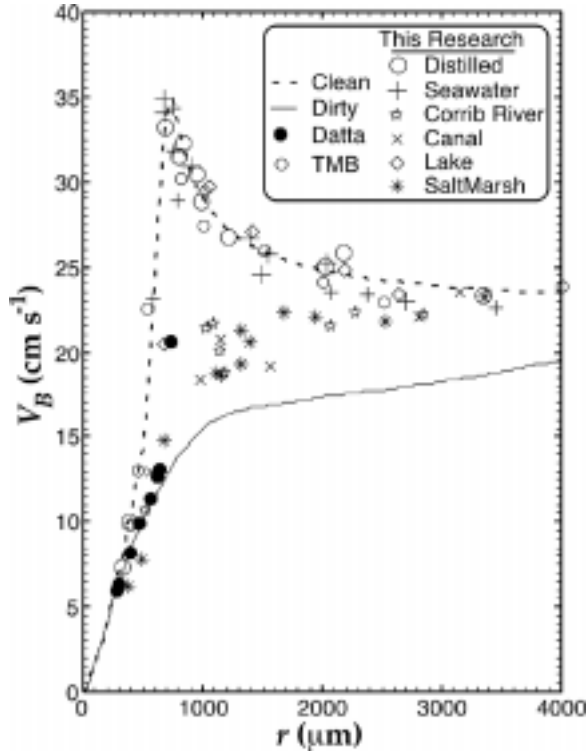


Figure 1. Rise velocity, V_B , as a function of radius, r , at 20°C from observations, other researchers, dirty parameterization from *Clift et al., [1978]*, and clean parameterization given by (1) and (3). Data key on figure. Datta - *Datta et al. [1950]*; TMB - *Haberman and Morton [1953]*. Collected waters were from the vicinity of Galway, Ireland (Lat: $53^\circ, 17'$; Long: $9^\circ, 3.6'$).

In contrast, the dirty V_B parameterization increases monotonically with r . Figure 1 also shows experimentally determined V_B for natural waters at room temperature ($19 - 21^\circ\text{C}$). The first water analyzed was seawater, and as shown in Figure 1 (crosses) V_B for bubbles in seawater was no more $1\text{-}2 \text{ cm s}^{-1}$ lower than that for distilled water and significantly greater than V_B dirty. Hypothesizing that perhaps this was a salinity effect, fresh lake water was analyzed and produced similar "clean" results. However, saltmarsh water showed a significant decrease from the clean V_B parameterization over a wide range of r , although

larger bubbles ($r > 2000 \mu\text{m}$) had V_B close to that of clean water. Canal water was also tested and V_B was found similar to the saltmarsh water.

The clean behavior of bubbles in seawater is surprising given the prevalence of surfactants in seawater [*Liss et al., 1997*]. It was hypothesized that these bubbles had not

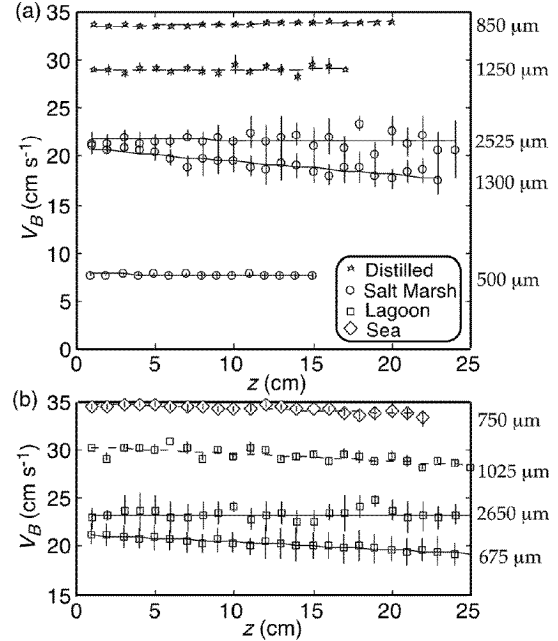


Figure 2. Rise velocity, V_B , versus height, z , above release depth, for bubbles of various sizes and waters. The legend for water type is on Figure 2a, bubble radii marked on figure.

Table 1. Coefficients for $V_B(z)$ regression analysis fit and its correlation coefficients of the fit.

$r(\mu\text{m})$	C	q	R^2
489	7.82	-0.009	0.69
677	21.46	-0.078	0.96
747	34.86	-0.047	0.83
1016	30.41	-0.74	0.79
1313	20.97	-0.139	0.91
2529	21.86	-0.008	0.08
2645	23.36	-0.0002	0.0003

achieved equilibrium and thus had accumulated insufficient surfactants to affect V_B . If true, V_B should decrease as a bubble rises, and in fact, this was the case. Figure 2 shows $V_B(z)$ segregated into 1-cm depth bins and averaged, where z is height above the capillary tube, and z increases towards the surface. Error bars are indicated by the length of the vertical lines determined by the standard deviation for all bubbles in each depth bin. Also shown the least-squares, linear-regression fit (i.e. $V_B = qz + C$, where q is slope and

C is the initial velocity) to each data set. The correlation coefficient, R^2 , q , and C are shown in Table 1. As can be seen in Figures 2a and 2b, smaller bubbles ($r < 500 \mu\text{m}$) become immobilized after rising less than 1 cm and hence there was no deceleration of V_B with z . As a result values of R^2 are small.

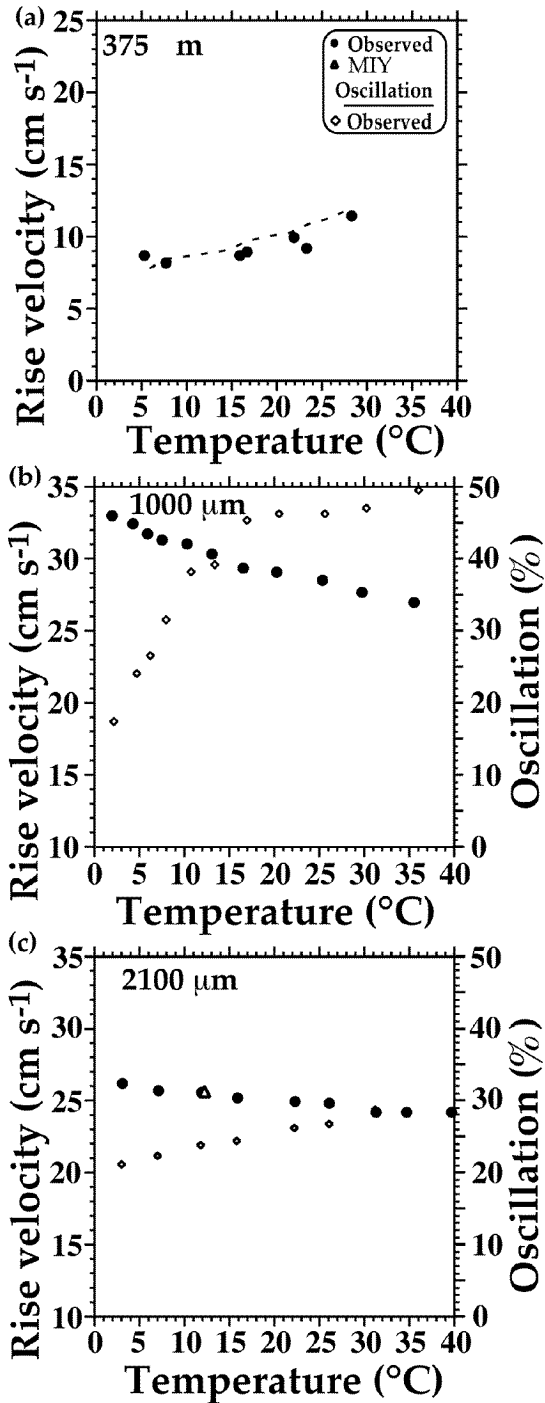


Figure 3. Observed temperature variation of bubble rise velocity for bubbles with radii (a) 375 μm , (b) 1000 μm , and (c) 2100 μm .

Also shown oscillation parameter in (%) where it applicable. MIY-Miyagi [1927].

In contrast, for intermediate ($600 < r < 2000 \mu\text{m}$) bubbles, V_B decreased as they rose. The high R^2 show the decrease in V_B is significant with z . This suggests that the bubbles become progressively dirtier as they rise and accumulate surfactants, and thus a greater percentage of the surface becomes immobilized. For very large bubbles ($r > 2500 \mu\text{m}$), the fluid flow around the bubble is much faster, bubble motions are more complex, and there is a decreased sensitivity to surfactants and low R^2 is small. Note that these size limits are approximate.

3.2. Temperature Dependence of V_B

Although bubble processes of geophysical interest occur in waters spanning a wide range of T , the effect of T on V_B has not been systematically studied. A series of experiments to measure $V_B(T)$ over the T range $0^\circ\text{C} - 40^\circ\text{C}$ was conducted in distilled water. It was observed that V_B increased with T for smaller bubbles and decreased for larger bubbles. Although for non-oscillating bubbles $V_B(T)$ could be explained by changes in viscosity and density, this is not true for oscillating bubbles. Furthermore, there was a strong relationship between V_B and ζ , the oscillation parameter, defined as V_B/V_x where V_x is the horizontal velocity. Figure 3 shows $V_B(T)$ and ζ for 375, 1000, and 2100 μm bubbles as well as observed Miyagi [1927].

The decrease in $V_B(T)$ for the oscillating bubbles suggests that energy from the buoyant rise is transformed into horizontal motions (i.e., trajectory oscillations) and shape oscillations. For the 1000- μm bubbles shown in Figure 3b, V_B decreased with T , while ζ increased from 19% at 3°C to a maximum of 50% at 36°C .

For significantly larger 2100- μm bubbles, V_B also decreased with T although less strongly. The decrease in the T dependency of V_B with increasing r is clearly shown by a comparison of the 2100- μm bubble results (Figure 3c) with the 1000- μm bubble results (Figure 3b). The decrease in the T dependency of V_B with increasing r is clearly mirrored in the T dependency of ζ . Changes in T cause much less change in ζ for 2100- μm bubbles (Figure 3c) than for smaller (i.e. 1000- μm) bubbles (see Figure 3b). Oscillations for the 2100- μm bubbles increased from the lowest observed temperature, 4°C to 31°C at which point they remained constant, although V_B continued to decrease with T .

At $T = 20^\circ\text{C}$, oscillations begin at approximately $r = 700 \mu\text{m}$, or $Re \sim 450$ [Clift et al., 1978] and V_B decreases with r ; however, at $Re \sim 1000$ ($r \sim 2000 \mu\text{m}$), path oscillations decrease, while bubble shape oscillations, especially higher modal oscillations, increase, and V_B no longer decreases with r .

4. DISCUSSION

In the natural environment, entirely clean surfaces are even less likely due to the presence of carbohydrates, proteins, fatty acids, [Liss *et al.*, 1997] and other organic and inorganic substances (note, salt is an ionic surfactant). The magnitude of the surfactant effect depends upon the surfactant kinetics and equilibrium surface concentration, C_s , as well as T and r . The observed size dependency of the surfactant effect in natural waters is in agreement with the trend for industrial surfactants where V_B decreased more for smaller bubbles [Okazaki, 1964].

In contaminated water, stress from the bubble's motion convects surfactants towards the downstream hemisphere, creating a gradient of C_s . This locally reduces the surface tension, σ , resulting in a tangential force towards regions of higher σ . Local surface viscosity is reduced causing decreased interfacial mobility. This interfacial retardation is called the Marangoni effect. Even for a contaminated interface, in the absence of gradients in σ , there is no Marangoni effect. Therefore, surfactants do not always cause a Marangoni effect. For example this occurs when surface diffusion is much faster than surface convection [Quintana, 1992]. Surfactant molecules diffuse from the bulk fluid to the new interface created at the upstream pole where $C_s < \alpha_s C_b$, where α_s is the surfactant surface solubility and C_b is bulk concentration. The surfactant is convected towards the downstream pole where it accumulates until $C_s > \alpha_s C_b$ and then desorbs and diffuses into the bulk fluid. The surfactant also diffuses against the surface convection towards the upstream hemisphere. Gradients in C_s are strongest in the downstream hemisphere, thus interface mobility is greater in the upstream hemisphere.

An analytic solution for the surfactant surface distribution and its effect on V_B , the Stagnant Cap Model, SCM, was developed by Sadhal and Johnson [1983], and is shown schematically in Figure 4. In the model, all the surface tension gradients occur across an immobilized cap in the downstream hemisphere. As a result, V_B is largely unaffected for increasing C_s until a stagnant cap angle of 30 to 45° is reached, at this point V_B decreases very rapidly for small increases in C_s . Once the cap extends above the equator, further growth once again has minimal effect on V_B . The SCM has been experimentally verified with industrial surfactants [Duineveld, 1995].

Based on the SCM, the simplest explanation for the "clean" behavior of bubbles in seawater is that they have not accumulated sufficient surfactant during their rise for the stagnant cap to extend greater than 30°. Since smaller bubbles have less surface area and lower convective forces, they accumulate surfactants more rapidly than larger bubbles. Thus V_B decreases more rapidly for smaller

bubbles as they rise. Very small bubbles achieved a fully developed stagnant cap after a few centimeters rise, and thereafter $V_B(z)$ was constant with z (Figure 2).

Ionic surfactants form a double layer at the interface which affects the bubble hydrodynamics [Borwanker and Wasan, 1988], and the Marangoni effect also becomes dependent upon ionic strength. This was experimentally verified by Fdihla and Duineveld [1996] for the ionic surfactant sodium dodecyl sulfate. Unlike non-ionic surfactants, the transition between clean and dirty was not rapid, but spread over a wide concentration range. The lack of a rapid transition in Figure 2 is far more suggestive of the effect of ionic surfactants than the SCM prediction. And of course saltwater contains ionic surfactants such as NaCl.

In natural waters the lowest V_B was for shallow waters, i.e., waters collected close to sediments. This suggests that surfactants from decomposition are much stronger than those from phytoplankton production. To test this hypothesis seawater was allowed to "age" in a glass tank in the sun and V_B was measured for 1000- μm bubbles every few days. No change was observed until the second week; when the water became the slightly yellow tinged, indicating plankton mortality, and V_B significantly decreased. It is likely that at this point algae began to decompose which may have been cause cell lysis, or bacterial exudation.

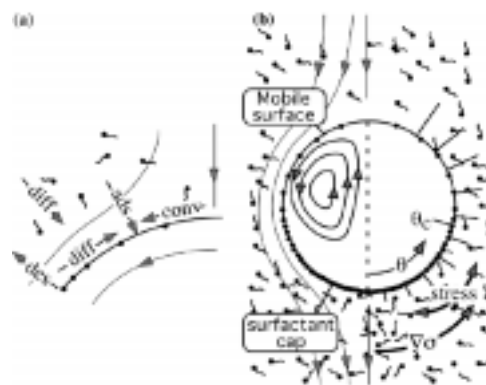


Figure 4. Schematic of Stagnant Cap Model for showing (a) the transport processes affecting surfactants on a bubble, and (b), the surface tension variation, σ , (radial line length) with zenith angle, θ . Key : ads- adsorption, des - desorption, diff - diffusion, conv - convection.

Although the experimental bubbles were produced from capillary tubes, there is strong reason to believe the results are applicable to oceanic bubbles. Wind-wave generated bubbles in bubble plumes were observed during the LUMINY experiment described in De Leeuw *et al.*, [2001] to burst immediately upon surfacing [Leifer and De Leeuw, 2001] a strong indication of bubble cleanliness [MacIntyre,

1972]. Presumably wave breaking and the bursting of surfacing bubbles sweeps away the surface microlayer [Leifer and De Leeuw, 2001]. Observations of the oscillations of oily bubbles rising from a natural hydrocarbon seep strongly indicated that larger ($r > 1500 \mu\text{m}$) bubbles do not become contaminated even after rising 70 m [Leifer, unpublished].

5. $V_B(T)$ PARAMETERIZATION

For spherical bubbles in laminar flow (i.e. $Re < 1$) the Navier-Stoke's equation can be solved analytically yielding the Hadamard-Rybczynski's solution for V_B for both mobile and immobile interfaces [Levich, 1962]. For larger, clean bubbles though, V_B diverges from the solution. Thus a power law modification of this equation was used to parameterized $V_B(r, T)$ for non-oscillating bubbles,

$$V_B = c \frac{1}{3} g r^d v^n \quad (1)$$

where c , d , and n are coefficients given in Table 2. Further details of the derivation can be found in Leifer et al. [2000].

For clean oscillating bubbles, V_B decreased with both increasing T and r , and a completely different analytic parameterization was developed. The onset of oscillation is not a simple function of Re but involves the shape since at different T , the onset occurs at different Re [Leifer et al., 2000]. The r for the onset of oscillation varies with T according to the relation

$$r_P = 1086 - 16.05 T_P \quad (2)$$

where r_P and T_P are peak r and T . Outside the observed range (7 - 26.8°C), (2) is presumably unreliable since, for example, it predicts $r_P = 0 \mu\text{m}$ for $T_P = 78^\circ\text{C}$, i.e., a zero radius bubble oscillates.

Table 2. Coefficients for Eqn. (1), the V_B parameterization for clean non-oscillating bubbles.

Re	r (μm)	c	d	n
<1	< 60	0.666	2.00	-1.00
1-150	60-500	0.139	1.372	-0.64
150-420	550-660	11.713	2.851	-0.64
420-470	660-700	0.156	1.263	-0.64
470-540	700-850	0.021	0.511	-0.64

For clean oscillating bubbles, the following empirical parameterization was developed from observation and is shown in Figure 1. It is in good agreement with Clift et al. [1978] at 20°C and is applicable for oscillating bubbles for $0 < T < 30^\circ\text{C}$ and $r_P < r < 4000 \mu\text{m}$, and is,

$$V_B = \{V_{Bm} + H(r - r_c)^{m_1} e^{\{K(r - r_c)^{m_2} T\}} \quad (3)$$

where H , K , m_1 and m_2 are coefficients, r_c is a critical radius below which the parameterization suggests bubbles do not oscillate for any T , and V_{Bm} is the minimum V_B for oscillating bubbles. Since (3) is analytical rather than empirical, the coefficients H and K do not have physical meaning. The coefficients are given in Table 3. A comparison between the parameterization (predicted) and observed values of V_B is shown in Figure 5. The correlation coefficient was 0.9455. The derivation of (3) can be found [Leifer et al., 2000].

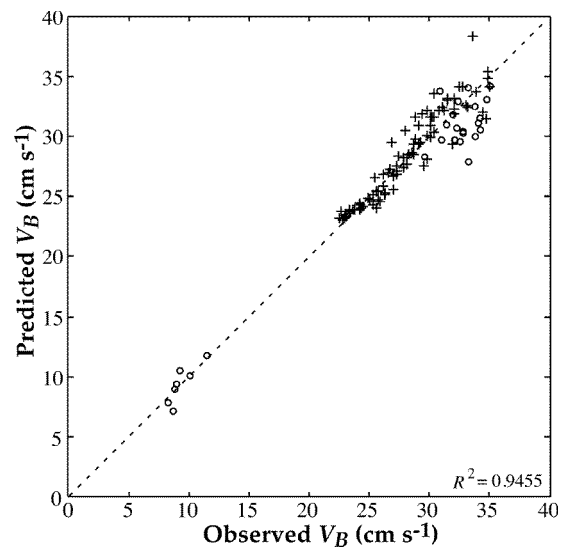


Figure 5. Comparison of parameterized and observed rise velocity, V_B , for oscillating bubbles (+). Also shown is predicted and observed V_B for non-oscillating 375 μm bubbles (o). The correlation coefficient, R^2 , was calculated only for oscillating bubbles.

Table 3. Coefficients for Eqn. (3), the V_B parameterization for clean oscillating bubbles.

H	K	r_c	V_{Bm}	m_1	m_2
-4.792×10^{-4}	0.733	0.0584	22.16	-0.849	-0.815

6. CONCLUSIONS

A study of bubble hydrodynamics for many fresh and salt waters, including seawater, showed that bubbles larger than approximately 600- μm radius behaved as though in distilled water. Bubbles in saltmarsh water and canal water, though, were found to have V_B values lower than those for clean bubbles, indicating surfactants had at least partially immobilized the bubble interface. Based on the data

presented in this paper, a reasonable approach to modeling shallow bubbles in seawater is to simulate small bubbles as dirty, and large bubbles as clean with a transition at circa 600 μm . However, the transition radius increases the longer the bubbles are in the water column.

An empirical parameterization of $V_B(r,T)$ for oscillatory and non-oscillatory bubbles that correctly incorporates the effect of T was presented. The parameterization is applicable to bubbles in clean freshwater. Additionally the parameterization should not be applied for $T > 40^\circ\text{C}$ or to other liquids. Since, V_B in seawater for large (i.e. oscillating) bubbles indicates that these bubbles are clean, it is reasonable to apply (3) to seawater. However, experimental verification is clearly required. Further investigation of the effect of surfactants on bubbles in natural waters is also clearly needed.

Finally, V_B is far more sensitive to the effect of surfactants than T . Since bubble gas transfer velocity, k_{Bub} , is a function of V_B , underestimates of V_B cause k_{Bub} to also be underestimated.

REFERENCES

- Borwanker, R.P. and D.T. Wasan, Equilibrium and dynamics of absorption of surfactants at the fluid/fluid interfaces. *Chem. Eng. Sci.*, 43, 1323-1337, 1988.
- Clift, R., J. R. Grace, and M. E. Weber, *Bubbles, Drops, and Particles*, Academic Press, New York, 1978.
- Datta, R.L., D.H. Napier and D.M. Newitt, The properties and behavior of gas bubbles formed at a circular orifice. *Trans. Inst. Chem. Eng.*, 28, 14-26, 1950.
- De Leeuw, G., G.J. Kunz, G. Caulliez, L. Jaouen, S. Badulin, D.K. Woolf, P. Bowyer, I. Leifer, P. Nightingale, M. Liddicoat, T.S. Rhee, M.O. Andreae, S.E. Larsen, F.Aa Hansen, and S. Lund, LUMINY - An Overview. In *Gas Transfer at Water Surfaces*, edited by M.A. Donelan, W.M. Drennan, E.S. Saltzman and R. Wanninkhof, pp. xxx-xxx, AGU, this volume, 2001.
- Duineveld, P.C., The rise velocity and shape of bubbles in pure water at high Reynolds number. *J. Fluid Mech.*, 292, 325-332, 1995.
- Fdhila, R.B., and P.C. Duineveld, The effect of surfactants on the rise of a spherical bubble at high Reynolds and Peclet numbers. *Phys. Fluids*, 8, 310-32, 1996.
- Haberman W.L., and R.K. Morton, An experimental investigation of the drag and shape of air bubbles rising in various liquids. *The David W. Taylor Model Basin.*, 55, Navy Dept., Washington 7 D.C, 1953.
- Jamialahmadi, M., C. Branch, and H. Müller-steinhausen, Terminal bubble rise velocity in liquids. *Trans. IChemE.*, 72A, 119-122, 1994.
- Leifer I., and De Leeuw, Bubble measurements in breaking-wave generated bubble plumes during the LUMINY wind-wave experiment. In *Gas Transfer at Water Surfaces*, edited by M.A. Donelan, W.M. Drennan, E.S. Saltzman and R. Wanninkhof, pp. xxx-xxx, AGU, this volume, 2001.
- Leifer I., R.K. Patro, and P. Bowyer, A study on the temperature variation of rise velocity for large clean bubbles. *J. Atm. Ocean. Tech.*, 17 (10), 1392-1402, 2000.
- Levich, V. G., *Physico-Chemical Hydrodynamics*, Prentice-Hall, Englewood Cliffs, N.J., 1962.
- Liss, P.S., A.J. Watson, E.J. Bock, B. Jähne, W.E. Asher, N.M. Frew, L. Hasse, G.M. Korenowski, L. Merlivat, L.F. Phillips, P.Schluessel, and D.K. Wolf, Physical processes in the microlayer and the air-sea exchange of trace gases. In *The Sea Surface and Global Change*, edited by P.S. Liss, and R.A. Duce, pp. 1-33, Cambridge University Press, Cambridge, UK, 1997.
- MacIntyre, F., Flow patterns in breaking bubbles. *J. Geophys. Res.*, 77, 5211- 5228, 1972.
- Medwin, H. and N.D. Breitz, Ambient and transient bubble spectral densities in quiescent seas and under spilling breakers. *J. Geophys. Res.*, 94C, 12, 571-12, 759, 1989.
- Miyagi-Kôgakuha-kusi, O., The motion of an air bubble in rising water. *Tohoku Imp. Univ. Tech. Reports*, V-VI, 135-171, 1927.
- Monahan, E.C., The ocean as a source for atmospheric particles. In *The Role of Air-Sea Exchange in Geochemical Cycling*, edited by P. Buat-Menard, pp. 129-163, D. Reidel Publishing Company, Hingham, Massachusetts, 1986.
- Okazaki, S., The velocity of ascending air bubbles in aqueous solutions of a surface active substance and the life of the bubble on the same solution. *Bull. Chem. Soc. Jpn.*, 37, 144-150, 1964.
- Quintana, G.C., The effect of surfactants on flow and mass transport to drops and bubbles. In *Transport Processes in Bubbles, Drops, and Particles* edited by R.P. Chhabra and D. De Kee, pp. 87-113, Hemisphere Pub. Corp., New York, 1992.
- Sadhil S., and R.E. Johnson, Stoke's flow past bubbles and drops partially coated with thin films. *J. Fluid Mech.*, 126, 237-250, 1983.
- Tsuchiya, K., H. Mikasa, and T. Saito, Absorption dynamics of CO₂ bubbles in a pressurized liquid flowing downward and its simulation in seawater. *Chem. Eng. Sci.*, 52, 4119-4126, 1997.

R. Patro, Physics Department, Memorial University of Newfoundland, St. John's, Canada, A1B3X7, (email: ranjan@physics.mun.ca).

I. Leifer, Chemical Engineering Department, University of California, Santa Barbara, Santa Barbara, California, 93106-5080, USA (email: ira.leifer@bubbleology.com).

P. Bowyer, National University of Ireland, Galway, Ireland, (email: peter.bowyer@nuigalway.ie).